

## MIT Open Access Articles

*The impact of negative selection on  
thymocyte migration in the medulla*

The MIT Faculty has made this article openly available. **Please share**  
how this access benefits you. Your story matters.

**Citation:** Le Borgne, Marie et al. "The Impact of Negative Selection on Thymocyte Migration in the Medulla." *Nature Immunology* 10.8 (2009): 823–830.

**As Published:** <http://dx.doi.org/10.1038/ni.1761>

**Publisher:** Nature Publishing Group

**Persistent URL:** <http://hdl.handle.net/1721.1/77963>

**Version:** Author's final manuscript: final author's manuscript post peer review, without publisher's formatting or copy editing

**Terms of use:** Creative Commons Attribution-Noncommercial-Share Alike 3.0



Published in final edited form as:

*Nat Immunol.* 2009 August ; 10(8): 823–830. doi:10.1038/ni.1761.

## The impact of negative selection on thymocyte migration in the medulla

Marie Le Borgne<sup>\*,†</sup>, Ena Ladi<sup>\*</sup>, Ivan Dzhagalov, Paul Herzmark, Ying Fang Liao, Arup K. Chakraborty<sup>#</sup>, and Ellen A. Robey

Division of Immunology, Department of Molecular and Cell Biology, University of California, Berkeley, CA 94720, USA

### Abstract

Developing thymocytes are screened for self-reactivity before exiting the thymus, but how thymocytes scan the medulla for self-antigens is unclear. Using two-photon microscopy, we observed that medullary thymocytes migrated rapidly and made frequent, transient contacts with dendritic cells. In the presence of a negative selecting ligand, thymocytes slowed, became confined to areas of approximately 30 microns in diameter, and had increased contact with dendritic cells surrounding confinement zones. One third of polyclonal medullary thymocytes also exhibited confined, slower migration, and may correspond to auto-reactive thymocytes. Our data suggest that many auto-reactive thymocytes do not undergo immediate arrest and death upon encounter with a negative selecting ligand, but rather adopt an altered migration program while remaining within the medullary microenvironment.

### Introduction

The thymic medulla is a crucial site for the elimination of T cells bearing auto-reactive T cell antigen receptors (TCRs), a process known as negative selection. The medulla is a specialized environment facilitating presentation of a wide array of self-antigens to developing thymocytes. One particularly remarkable specialization is the expression of “tissue restricted antigens” (TRAs), such as insulin, in a subset of medullary epithelial cells, a phenomenon that has been termed “promiscuous gene expression”<sup>1</sup>. The importance of this mechanism for maintaining self-tolerance is illustrated by the effect of mutation of the transcriptional regulator AIRE (autoimmune regulator) that leads to a loss of tissue restricted gene expression in medullary epithelial cells and results in organ-specific autoimmune disease due to the failure to eliminate auto-reactive T cells in the thymus<sup>2, 3</sup>.

A number of different cell types play roles in presenting self-antigens to developing T cells in the medulla. Medullary thymic epithelial cells (mTECs) express TRAs<sup>4</sup> leading to the elimination of self-reactive thymocytes<sup>5, 6</sup>, and can present these antigens to CD8 medullary thymocytes<sup>7</sup>. Thymic dendritic cells (DCs) bring peripheral antigens into the thymus<sup>8, 9</sup>, and cross-present AIRE-dependent antigens to both CD4 and CD8 T cells<sup>7</sup>.

Correspondence should be addressed to E.A.R. (erobey@berkeley.edu).

<sup>\*</sup>equal co-authors

<sup>#</sup>Department of Chemistry, Department of Chemical Engineering and Department of Biological, Engineering, Massachusetts Institute of Technology, Cambridge, MA 02139, USA

<sup>†</sup>current address: Department of Pathology and Immunology, Washington University School of Medicine, St Louis MO 63110, USA

### Author contributions

M.L.B. and E.L. designed and performed experiments, analyzed and interpreted results, and wrote the manuscript; I.D. analyzed FoxP3-GFP<sup>+</sup> cell migration; P.H. provided technical support for imaging; Y.F.L. did manual scoring and tracks editing; A.C. provided guidance for quantitative analysis of cell migration data; and E.R. directed the study and wrote the manuscript.

Interestingly, mTECs in adult mice undergo rapid turnover, and AIRE expression promotes the death of the most mature mTEC populations<sup>10</sup>. The death of AIRE-expressing mTECs may contribute to the cross-presentation of TRAs by DCs<sup>7, 11</sup>. Given that only a fraction of mTECs expresses any given TRA<sup>4</sup>, cross-presentation of these antigens by DCs may help to increase the spatial distribution of TRAs in the medulla and make it more likely that auto-reactive thymocytes will encounter cognate self-antigen during the four days that they spend in the medulla<sup>12</sup>.

Much of our information about negative selection in the medulla comes from analysis of dissociated thymocyte populations, and many key questions about the spatial and temporal aspects of negative selection remain unanswered. How do medullary thymocytes migrate and interact with potential antigen presenting cells (APCs) during the four to five days they spend in the medulla<sup>12</sup>? Are there anatomical niches in the medulla in which negative selection occurs? Do thymocytes undergo immediate arrest and cell death upon encounter with a negative selecting ligand, or is there first a period of transient contacts, as has been proposed for mature T cell priming in lymph nodes<sup>13</sup>? Do thymocytes that are receiving negative selection signals make up a significant proportion of steady state medullary thymocytes? Two-Photon Laser Scanning Microscopy (TPLSM) provides the opportunity to observe cell migration and cellular interactions within 3-dimensional tissue environments and thus is an important tool to address these questions<sup>14, 15</sup>. Although this approach has been used to examine the thymic cortex<sup>16–19</sup>, the technical challenges of imaging the deeper regions of tissues have thus far precluded time-lapse imaging of the thymic medulla.

Here, we overcame those technical challenges to investigate thymocyte migration and thymocyte-DC interactions in the medulla. We found the migration of medullary thymocytes to be confined and more rapid than that of cortical thymocytes, and we noted that medullary thymocytes make frequent and transient contacts with DCs. Using a model for AIRE-dependent negative selection in the medulla<sup>5</sup>, we showed that in the presence of a negative selecting ligand, thymocytes migrated more slowly and in a highly confined manner within zones of ~30 microns in diameter. Within these confinement zones, auto-reactive thymocytes continued to make transient contacts with multiple DCs, although their interaction time with DCs was significantly higher compared to thymocytes in the absence of their negative selecting ligands. Within polyclonal thymocyte samples, we identified a population of slow-migrating thymocytes exhibiting a highly confined migration pattern, which likely represents auto-reactive thymocytes that are fated for negative selection. These results provide new insights in the cellular dynamics and interactions that lead to negative selection in the medulla.

## Results

### Imaging the medulla in a cut-thymus preparation

The thymic medulla is generally more than 200  $\mu\text{m}$  under the capsule of the thymus, just at the limit of detection by TPLSM. To reliably image in the medulla, we have developed a modified version of a published protocol<sup>17</sup> in which an isolated thymic lobe is embedded in agarose, cut in half along the sagittal plane using a vibratome, and imaged through the cut site (Supplementary Fig. 1). We used reporter mice in which the DC-specific CD11c promoter drives YFP expression<sup>20</sup>, and we injected mice just prior to sacrifice with fluorescent lectin to label the blood vessels. The medulla can be readily distinguished from the cortex, based on its high density of YFP<sup>+</sup> cells (30,000–50,000 cells/ $\text{mm}^3$  versus 15,000–20,000 cells/ $\text{mm}^3$  in the cortex), and size and orientation of blood vessels at the cortical-medullary junction (CMJ) (Fig. 1a).

To introduce fluorescently labeled thymocytes, we generated partial hematopoietic chimeras using bone marrow (BM) from donor transgenic mice that express GFP under the control of the ubiquitin promoter (ubiGFP)<sup>21</sup> or CFP under the control of the actin promoter (actinCFP)<sup>22</sup> as donors, and CD11c-YFP reporter mice as hosts. Some donor mice also carried a MHC class I (MHC-I) restricted rearranged TCR transgene (OT1 TCR or P14 TCR), which allowed comparison of thymocytes with a defined positive selecting TCR to polyclonal thymocytes (non TCR transgenic: here designated wild-type or WT). In these chimeras, donor-derived thymocytes made up 0.2 – 1% of total thymocytes, and displayed a CD4/CD8 profile similar to that of donor mice<sup>18, 19</sup> (and data not shown).

To confirm that vibratome sectioning does not drastically alter the physiology of the thymus, we compared data from the cortex of cut thymic lobe preparations to intact thymic lobes<sup>23</sup>. As in intact thymic lobes<sup>19</sup>, the dendrites of DCs in cut thymic preparations underwent constant probing motions while their cell bodies remained stationary (Supplementary Movie 1). The average speeds of polyclonal and TCR transgenic thymocytes were not significantly different in cut thymic lobes versus intact thymic explants (Fig. 1b). As previously reported in intact thymic lobes, increased positive selection in cut TCR transgenic thymi correlated with an increase in the average thymocyte speed (Fig. 1b)<sup>18</sup>. Overall, these results show that our sectioning protocol does not grossly affect the behavior of DCs or the motility of thymocytes.

### Rapid, confined medullary thymocyte migration

Based on previous work that established a relationship between positive selection and increased migration speed, and the faster speed of lymph node T cells compared to cortical thymocytes<sup>18, 24</sup>, we might expect medullary thymocytes, which have undergone positive selection, to migrate faster than cortical thymocytes. Indeed, medullary thymocytes migrated significantly faster than cortical thymocytes (Fig. 2a,b and Supplementary Movie 1) in both polyclonal and TCR transgenic systems.

Cortical thymocytes migrate *via* random walk and, upon receiving positive selection signals, migrate directionally towards the medulla<sup>18</sup>. To determine if medullary thymocytes migrate randomly, we plotted the mean displacement of thymocytes from their origin as a function of the square root of time for each imaging volume. For the cortex, these plots were linear, indicating random migration, consistent with previous reports (Fig. 2c)<sup>17, 18</sup>. In contrast, while medullary thymocytes exhibited random walk over relatively short time scales (4–9 minutes), the plots eventually reach a plateau indicating that their migration is confined<sup>14</sup> (Fig. 2c). The plateau value, which indicates the confinement distance (red dotted lines, Fig 2c), showed considerable run-to-run variation (ranging from 25 to 67 microns; Supplementary Fig. 2a) and was not significantly affected by proximity to the cortical medullary junction (data not shown). The instantaneous speed of thymocytes showed no overall decrease with time, even when followed for two successive runs from the same thymic lobe (Supplementary Fig. 2b), ruling out that the plateaus were due to gradual decrease in thymocyte motility during the experiment. As expected based on the average speeds (Fig. 2b), the motility coefficient, as determined from the slope of these limited random-walk regions (black dotted line in Fig. 2c), was higher in the medulla compared to the cortex (Supplementary Fig. 2c).

Visual inspection revealed regions in the medulla that are devoid of thymocyte tracks, a phenomenon that was most apparent in runs containing larger numbers of labeled thymocytes (Supplementary Fig. 2d). In addition the “straightness ratio”, defined here as the maximal displacement divided by the total length of the path, was consistently lower for medullary thymocytes when compared to cortical thymocytes of comparable speeds

(Supplementary Fig. 2e). Taken together, these data indicate that medullary thymocytes do not freely migrate through the medulla but rather follow confined migratory paths.

### Negative selection alters speed and confinement

To determine the impact of negative selection on medullary thymocyte migration, we employed the RIPmOVA-OT1 system. In this system a membrane-bound form of the model antigen ovalbumin (OVA) is expressed under the control of the rat insulin promoter (RIP) in the pancreatic islets as well as medullary thymic epithelial cells<sup>5, 7, 25</sup>, and T cells express a rearranged TCR transgene (OT1) specific for OVA peptide presented in the context of MHC-I, K<sup>b</sup>. Deletion in this system spares the majority of CD4<sup>+</sup>CD8<sup>+</sup> thymocytes, but leads to the loss of the most mature CD8<sup>+</sup>CD4<sup>-</sup> single positive (SP) thymocytes and a population of CD4<sup>+</sup>CD8<sup>int</sup> thymocytes<sup>5,7</sup>; the latter were proposed to be a transitional population that is becoming SP<sup>26, 27</sup>. To confirm and extend these observations in a recombination activating gene (RAG)-deficient background, we compared the thymuses of OT1 *Rag2*<sup>-/-</sup> RIPmOVA<sup>-</sup> (here designated “OT1”) and OT1 *Rag2*<sup>-/-</sup> RIPmOVA<sup>+</sup> (here designated “OT1 RIPmOVA”) littermates. Although there were no significant differences in overall thymic cellularity ( $64 \pm 18$  versus  $65 \pm 18 \times 10^6$  cells/thymus respectively), there was a significant reduction in the percentage of CD8 SP and CD4<sup>+</sup>CD8<sup>int</sup> thymocytes (Supplementary Fig. 3a). To identify the thymocyte populations that are undergoing apoptosis, we used an antibody for the active form of caspase 328. We found a significant increase in the proportion of active-caspase 3<sup>+</sup> cells in both the CD4<sup>+</sup>CD8<sup>int</sup> and CD8 SP subsets of OT1 RIPmOVA compared to OT1 thymocytes (Supplementary Fig. 3b). Although a substantial number of CD4<sup>+</sup>CD8<sup>+</sup> thymocytes remained in OT1 RIPmOVA mice, there was a >90% reduction in both the number and percentage of the most mature V $\alpha$ 2<sup>+</sup> CD24<sup>-</sup> CD4<sup>+</sup>CD8<sup>+</sup> thymocytes (Supplementary Fig. 3c and data not shown). There was also a marked reduction in the number and percentage of CD8 T cells in the lymph nodes (Supplementary Fig. 3d). Together these data indicate that deletion occurs relatively late in this system of negative selection, but ultimately leads to the efficient removal of auto-reactive CD8 T cells in the thymus.

To image thymocyte migration in a negative selecting environment, we generated partial BM “co-chimeras” with mixtures of BM from wild-type CFP and OT1 GFP mice injected into RIPmOVA CD11c-YFP<sup>+</sup> double transgenic hosts (WT+OT1→+OVA). For comparison, we also generated chimeras using RIPmOVA<sup>+</sup>CD11c-YFP<sup>+</sup> littermates as hosts (WT+OT1→-OVA). In chimeras with the RIPmOVA transgene, we saw a reduction in CD4<sup>+</sup>CD8<sup>int</sup> OT1 thymocytes relative to those without the RIPmOVA transgene (Supplementary Fig. 4a) similar to the results from the OT1 RIPmOVA double transgenic mice (Supplementary Fig. 3a). Two-photon imaging of cut thymic lobes from chimeric mice revealed that the ratio of OT1 thymocytes in the medulla compared to the cortex was two fold lower in hosts with the RIPmOVA transgene, compared to those without OVA (Supplementary Fig. 4b), consistent with flow cytometric analysis of thymocytes from OT1 RIPmOVA mice (Supplementary Fig. 3). The average speed of medullary OT1 thymocytes was significantly lower in the presence of OVA (Fig. 3a,b and Supplementary Movie 2) whereas the speed of medullary wild-type thymocytes was not significantly affected by the expression of OVA (data not shown). OT1 thymocytes consistently migrated more slowly than wild-type thymocytes in +OVA hosts when compared within the same imaging volumes, whereas they were slightly faster than wild-type thymocytes in the absence of OVA (Fig. 3c). The speed of OT1 thymocytes in the cortex was not significantly different in hosts that did or did not express the OVA transgene (Fig. 3b), as expected based on the expression of the transgene in the medulla<sup>5, 7</sup>

In addition to labeled medullary thymocytes, donor-derived DCs were also found in the medulla, but could be distinguished from thymocytes by their size and morphology (Fig. 2a, white arrows; Supplementary Movie 1). To confirm that the reduction in thymocyte speed during negative selection was not attributable to the donor-derived DCs that might have been erroneously identified as thymocytes, we generated chimeras using OT1 GFP donors that also express the diphtheria toxin receptor (DTR) under the control of the CD11c promoter<sup>29</sup> and depleted these donor-derived GFP<sup>+</sup> DCs with diphtheria toxin injections before imaging (Supplementary Fig. 5a). The speed of the OT1 thymocytes in the medulla of these chimeras was not significantly different than in chimeras in which donor-derived DCs were not depleted (Fig. 3b,  $P > 0.05$ ) and was substantially lower than that of wild-type thymocytes in the same experiments (Supplementary Fig. 5b,  $P < 0.001$ ). These data confirm that medullary OT1 thymocytes exhibit reduced speed in the presence of their negative selecting ligand.

In addition to reduced speed, auto-reactive OT1 thymocytes exhibited a highly confined migration pattern. This can be seen from plots of the average displacement from origin against the square root of time, as well as by visual inspection of thymocyte tracks (Fig. 3d and Supplementary Movies 2 and 3). The average confinement distance for auto-reactive OT1 thymocytes ( $30 \pm 2.5 \mu\text{m}$ ) was significantly lower than for wild-type thymocytes from the same imaging volumes ( $55 \pm 20 \mu\text{m}$ ) and for OT1 thymocytes in the absence of OVA ( $52 \pm 17 \mu\text{m}$ ) (Fig. 3e). Visual inspection of the tracks of auto-reactive OT1 thymocytes revealed distinct “confinement zones” within an imaging volume whose dimensions were consistent with the confinement distances as determined by graphs of average displacement (Fig. 3d, Supplementary Movie 3).

To estimate how long auto-reactive thymocytes remained within confinement zones, we identified 67 individual thymocyte tracks within 17 distinct zones and followed them over the course of the imaging runs (Supplementary Movie 4). Fifty-six out of 67 thymocytes remained within a single confinement zone for as long as they remained in the imaging volume or duration of the run (average imaging time: 13 min/track) (Fig. 3f). Six out of 67 thymocytes were seen leaving a zone, and 9 were seen entering a zone (Fig. 3f and Supplementary Movie 4). Extrapolating from the number of cells observed leaving the zones, and assuming first order decay kinetics, we estimated a half-life of 1.6 hours for auto-reactive thymocytes to remain within a single confinement zone. We also noted that out of the 67 thymocytes, 26 migrated out of the imaging volumes but the majority were still visible at the end of the run, and only one seemed to disappear while within the confinement zone (Fig. 3f). This suggests that cell death and engulfment are infrequent occurrences for auto-reactive thymocytes within confinement zones.

### Thymocyte-DC interactions during negative selection

While OVA expression in RIPmOVA transgenic mice is limited to a subset of mTECs, BM-derived cells, presumably DCs, can cross-present OVA to OT1 thymocytes and induce their negative selection<sup>7</sup>. The zones defined by auto-reactive thymocyte migration were generally located between the bodies of DCs (Fig. 3d and Supplementary Movie 5), implying that auto-reactive thymocytes did not form lengthy interactions with individual DCs, but could have contacted multiple DCs during migration within a confinement zone. The vast majority (>98%) of CD11c-YFP<sup>+</sup> cells in the medulla were non-motile, in agreement with previous observations<sup>19</sup>.

In general the contacts between thymocytes and DCs in the medulla were short and dynamic, with thymocytes often contacting several DCs successively (Fig. 4, Supplementary Table 1, and Supplementary Movies 6,7). In the presence of OVA, OT1 thymocytes



interacted more extensively with DCs (Fig. 4a–c, Supplementary Table 1, and Supplementary Movie 6,7), although contacts remained brief and did not correspond to a decrease in instantaneous speed (data not shown). The slight increase in the average duration of contacts (1.9 in +OVA versus 1.2 minutes in –OVA environments), together with the slightly increased frequency of the contacts (6.8 versus 5.5 contacts per hour), resulted in a 2 fold increase in the total time that auto-reactive OT1 thymocytes spent in contact with DCs in the presence compared to in the absence of OVA (Fig. 4a–c and Supplementary Table 1). We also compared the DC contacts of OT1 versus wild-type polyclonal thymocytes in the same imaging volumes to control for local variations in DC density (Fig. 4d). In the presence of OVA, OT1 thymocytes consistently spent more time interacting with DCs compared to wild-type thymocytes in the same imaging volumes, whereas the contacts were similar when the host did not express OVA (Fig. 4d, Supplementary Table 1). Together, these data indicate that auto-reactive OT1 thymocytes exhibit increased interactions with DCs, reflecting successive contacts with multiple DCs surrounding zones of confined migration.

### A slow, confined population of polyclonal medullary thymocytes

Polyclonal medullary thymocytes represent cells that have been positively selected, and might be expected to resemble medullary thymocytes expressing a defined positive selecting TCR. We were therefore surprised to note that wild-type polyclonal medullary thymocytes, but not TCR transgenic thymocytes in positive selecting environments, contained a distinct population of more slowly migrating cells (Fig. 2b and Fig. 5a). The observation that the average speed of OT1 thymocytes was lower in the presence of their negative selecting ligand (Fig. 3b–c) suggested that the slower population in wild-type samples may represent auto-reactive thymocytes that are in the process of undergoing negative selection.

If the slow polyclonal population represents auto-reactive thymocytes, we might expect these cells to be present in both MHC-I restricted (CD8) and MHC-II restricted (CD4) thymocyte populations. To examine this possibility, we generated partial BM chimeras using mice transgenic for GFP or CFP that were otherwise wild-type as donors, and MHC-I or MHC-II deficient mice as hosts (WT→MHC-I<sup>−/−</sup>, or WT→MHC-II<sup>−/−</sup>). MHC-I and MHC-II restricted medullary thymocytes displayed an overall similar distribution of speeds as polyclonal thymocytes (mean average speeds of 14.9 μm/min and 13.0 μm/min, respectively) with the majority of cells migrating rapidly, and a distinct population of cells migrating at average speeds of less than 8 μm/min (Fig. 5a). These data indicate that both CD4 and CD8 medullary thymocytes contain a distinct population of more slowly migrating cells which may correspond to auto-reactive thymocytes.

Regulatory T (T<sub>reg</sub>) cells expressing the transcription factor Foxp3 are present amongst polyclonal medullary thymocytes, but are generally absent when selection is limited to a defined positive selecting TCR30. To test the possibility that the slow population in medullary polyclonal thymocytes corresponds to T<sub>reg</sub> cells, we imaged reporter mice in which the expression of GFP is controlled by the promoter of *Foxp3*. GFP<sup>+</sup> cells in the medulla displayed a distribution of speeds very similar to that of polyclonal MHC-II restricted thymocytes, with a mean average speed of 12.8 μm/min (Fig. 5a,b). These data rule out the possibility that the population of slow medullary thymocytes corresponded exclusively to Foxp3<sup>+</sup> T<sub>reg</sub> cells.

If the slower polyclonal medullary thymocyte population corresponded to auto-reactive thymocytes, we might expect them to display more confined migration resembling that of OT1 thymocytes in the presence of OVA. To test this prediction, we separated wild-type thymocyte tracks based on their average speeds (<8 μm/min and >8 μm/min) and estimated the confinement distances for each population (Fig. 5c,d). The slower wild-type medullary

thymocytes migrated in smaller confined regions than faster wild-type cells ( $22 \pm 4 \mu\text{m}$  vs  $54 \pm 9 \mu\text{m}$ ; Fig. 5c,d), and displayed similar confinement to auto-reactive OT1 thymocytes (Fig. 3e, 5c). This was most striking when comparing slower wild-type tracks to the tracks of auto-reactive OT1 thymocytes in the same imaging volumes (Fig. 5c and Supplementary Movie 8). Moreover, the tracks of slower wild-type thymocytes could be assigned to distinct confinement zones, which were similar to, and occasionally overlapped with, those of OT1 auto-reactive thymocytes. (Fig. 5c and Supplementary Movie 8). This population with highly confined migration likely accounts for the overall decrease in average confinement distance of wild-type thymocytes compared to OT1 and P14 thymocytes in positive selecting environments (Supplementary Fig. 2a). Thus polyclonal thymocytes contain a subset of cells that displays a similar migration profile to autoreactive OT1 thymocytes, and likely represents cells that are undergoing negative selection in the medulla.

## Discussion

Thymocytes bearing TCRs that recognize antigens expressed by medullary epithelial cells are eliminated by negative selection, but how thymocytes scan the medulla for negative selecting ligands, and the cellular dynamics of thymocyte-antigen presenting cell interactions during negative selection are not known. Here, we used two-photon imaging to address these questions. We found that medullary thymocytes move rapidly compared to cortical thymocytes, undergo confined migration, and make frequent, transient contacts with DCs. Auto-reactive thymocytes became further confined in their migration and migrated more slowly, making more extensive contacts with DCs that surrounded the confinement zones. Our data are consistent with a model in which some auto-reactive thymocytes do not undergo immediate arrest and cell death upon encountering their negative selecting ligands, but continue to scan potential antigen presenting cells in a local region of the medulla.

In the absence of negative selection, the average speed of medullary thymocytes ( $15 \mu\text{m}/\text{min}$ ) is comparable to that of mature T cells in the lymph node<sup>14,24</sup>. Previous observations showing that positive selection correlates with increased speed of cortical thymocytes, and that the fastest cortical thymocytes are migrating directionally toward the medulla<sup>18</sup>, suggest that the increased speed of medullary thymocytes is part of the developmental program induced by positive selection. The high speed of medullary thymocytes contributes to their ability to contact multiple DCs, estimated at about 500 DCs total during the four days they spend in the medulla<sup>12</sup>. However this may be an overestimate of the total number of individual DCs contacted, since the confined migration pattern of medullary thymocytes means that they may contact the same DC multiple times before migrating to another region.

In the presence of negative selecting ligand, medullary thymocytes moved more slowly, were more confined in their migration, and formed frequent and slightly prolonged contacts with DCs that surround the region of confined migration. Two-photon studies of lymph nodes have led to the notion of two phases of T cell priming; a first stage dominated by transient contacts with DC and a second stage characterized by stable interactions, with the first transient phase most prominent when TCR stimulation is suboptimal<sup>13, 32</sup>. It is tempting to speculate that the transient interactions of auto-reactive thymocytes with DCs reported here may serve as phase one of negative selection, perhaps allowing thymocytes to confirm that they are auto-reactive before becoming committed to die. The slightly increased duration of contacts with DCs in the presence of the negative selecting ligand is consistent with this notion.

At first glance it seems surprising that thymocytes undergoing apoptosis were not a prominent feature of this model of negative selection. However, very few dying cells are detected in the thymus of adult mice, perhaps due to the efficient engulfment and removal of



apoptotic thymocytes by macrophages<sup>33</sup>. Moreover, it seems likely that auto-reactive OT1 thymocytes persist in the medulla for days before dying, based on the estimates of 4 day dwell time in the medulla<sup>12</sup>, and the approximately 50% reduction in the number of medullary thymocytes in this model of negative selection. Thus hundreds of hours of cumulative imaging time for OT1 thymocytes in RIPmOVA hosts would be needed to record numerous examples of thymocyte death, rather than the ~24 hours of cumulative imaging time reported here. In addition, it is possible that the difficulty in observing thymocyte arrest and death in this negative selection model may reflect the low amount of self-antigen present in the AIRE-dependent form of negative selection; other forms of negative selection may proceed more rapidly. Indeed, the observation that superantigen-mediated deletion leads to the efficient removal of forbidden V $\beta$ s from the repertoire of mature CD4<sup>+</sup>CD8<sup>-</sup> and CD4<sup>-</sup>CD8<sup>+</sup> thymocyte subsets<sup>34</sup> implies that negative selection occurs more rapidly in this setting.

It is worth considering these findings in light of what is known about the distribution of self-antigens in the medulla. Contact with five DCs per hour would likely be more than adequate to eliminate thymocytes that are specific for broadly expressed self-antigens. However, any given TRA may be expressed by only 0.5% to 2% of mTECs<sup>4</sup> and thus may be quite restricted in its anatomical distribution in the medulla. While cross-presentation by DCs may broaden the distribution of TRAs somewhat, the observation that DCs are generally sessile in the thymus<sup>19</sup> and this manuscript means that thymocytes must migrate in the vicinity of an mTEC that expresses the cognate self-antigen in order to be negatively selected. Moreover, it seems likely that the amount of TRA presentation may also be limiting, given that TRA expression on mTECs is low relative to the expression of the same antigen in peripheral tissues<sup>35</sup>, and that an antigen may also have to make its way from an mTEC to a DC for cross-presentation. Thus, the requirement for a thymocyte to be able to respond to very low antigen concentration may be as important as the total number of DCs that can be scanned. In this regard, a scanning strategy in which thymocytes respond to a weak TCR signal by migrating in a confined area near the initial site of antigen contact could increase the chances that a thymocyte will re-encounter a self-antigen, thereby making the sampling of potential antigen-presenting cells more efficient.

It is unclear what anatomical features characterize the confinement zones of auto-reactive thymocytes. The average diameter of ~30  $\mu$ m for a confinement zone is consistent with the possibility that confinement occurs due to the tethering of migrating auto-reactive thymocytes to a large antigen-presenting cell. Although there is evidence that DCs can cross-present antigen to OT1 T cells in this system<sup>7</sup>, migration along the surface of a DC cannot account for the confined migration of auto-reactive thymocytes reported here, because confinement zones are found in between, not surrounding, the cell bodies of individual DCs. Medullary epithelial cells can also present directly to OT1 thymocytes in this system<sup>7</sup>, and it is possible that one or a group of OVA-expressing mTECs could define a confinement zone. Another intriguing possibility is that confinement zones correspond to the sites of recent demise of an OVA-expressing mTEC. This possibility is suggested by recent evidence that mTECs turn over rapidly, and that AIRE expression promotes the death of the most mature mTECs<sup>10</sup>. If antigens from dying mTECs become available for cross-presentation by nearby DCs, this could lead to the positioning of DCs presenting TRAs close to thymocytes that are deciding whether to undergo negative selection.

Perhaps the most surprising aspect to this study is the evidence that a substantial proportion of steady-state polyclonal medullary thymocytes display a migration signature indicative of negative selection. These data are consistent with the view that a substantial proportion of polyclonal thymocytes remain viable and motile for some time after they encounter negatively selecting ligands. The notion that thymocytes may encounter a negative selecting

ligand and not be rapidly eliminated is also consistent with recent observations in a system for negative selection in the cortex<sup>28, 36</sup>, and makes sense in light of recent observations that auto-reactive medullary thymocytes provide signals for the maturation of mTECs<sup>37–39</sup>. The persistence and confined migration patterns of thymocytes undergoing negative selection may reflect their ongoing interactions with other cells as they help to construct and maintain medullary niches specialized in negative selection.

## Methods

### Mice

All mice were housed and bred in pathogen-free conditions at the AALAC approved animal facility at Life Sciences Addition of University of California, Berkeley. All animal experiments were approved by the Animal Care and Use Committee of UC Berkeley. C57BL/6 (B6) mice (Jackson Labs) were crossed to CD11c-YFP transgenic mice on a B6 background<sup>20</sup> for use as neonatal hosts to generate partial hematopoietic chimeras as described previously<sup>18, 23</sup>. RIPmOVA transgenic mice on a B6 background<sup>25</sup>, provided by Mark Anderson (UCSF), were crossed to CD11c-YFP mice for use as neonatal hosts in some experiments. BM donors were either UBI-GFP transgenic mice<sup>40</sup>, or UBI-GFP mice crossed several times to OT1 TCR transgenic *Rag2*<sup>−/−</sup> mice (Taconic) or P14 TCR transgenic *Rag2*<sup>−/−</sup> mice (Taconic). In addition, OT1 TCR, UBI-GFP double transgenic *Rag2*<sup>−/−</sup> mice were crossed to CD11c-DTR mice to make OT1 TCR, UBI-GFP, CD11cDTR triple transgenic *Rag2*<sup>−/−</sup> donors. Co-chimeras were generated using actin-CFP transgenic B6 donors<sup>22</sup>. *MHC-I*<sup>−/−</sup> (*β2microglobulin*<sup>−/−</sup>) and *MHC-II*<sup>−/−</sup> (*H2-Aβ*<sup>−/−</sup>) mice (Taconic) were used as neonatal hosts. OT1 *Rag2*<sup>−/−</sup> mice crossed to RIPmOVA mice were used to generate OT1<sup>+</sup> *Rag2*<sup>−/−</sup> RIPmOVA<sup>+</sup> mice. Foxp3-GFP transgenic mice<sup>31</sup> were purchased from Jackson Labs.

### Two-Photon Imaging

At 4 to 6 weeks of age, chimeric mice were injected *via* tail vein with 100–200 μg of lectin-Texas Red (Vector Labs) just prior to sacrifice<sup>19</sup>. Cut thymic lobe preparations presented here are based on the modification of a previously described protocol<sup>17</sup>. Briefly, individual thymic lobes were embedded in low-melting-temperature agarose and sectioned with a Vibratome in two halves along the sagittal plane. Intact thymic lobes or cut thymic lobes were imaged by Two-Photon Laser Scanning Microscopy while being perfused with warmed, oxygenated medium as described previously<sup>19</sup>. Imaging volumes of 171 × 143 × 60–80 μm<sup>3</sup> were scanned every 25 seconds for 15–30 minutes using a custom-built microscope with a Spectra-Physics MaiTai Laser tuned to 900nm for excitation of CFP, GFP, and YFP and TexRed and separation of emission spectra using 495nm, 510nm and 560nm dichroics as well as 450/80nm and 645/75nm band-pass filters (Chroma). The imaging volumes were at least 30 μm under the cut site for cut thymuses or 80 μm under the surface of the capsule for intact thymic lobes. Individual imaging volumes were assigned to cortex or medulla based on the density of DCs and the location and orientation of large blood vessels at the cortico-medullary junction. Imaging volumes where this assignment was ambiguous were excluded from the analysis. For the chimeras using MHC-I and MHC-II deficient hosts, in which DCs were not labeled, the medulla was identified based exclusively on the blood vessel pattern.

### Data Analysis

The *x,y,z* co-ordinates of individual thymocytes over time were obtained using Imaris Bitplane Software and motility parameters were calculated using MATLAB (Mathworks Inc., Boston; code available upon request), and graphed using GraphPad Prism. Speed was defined as pathlength divided by time (μm/min). Straightness ratio was defined as the

maximum displacement divided by the total length of the path. Random walk analysis for each imaging volume was performed by plotting the average displacement from origin of the thymocytes in the volume against the square root of time<sup>14</sup>. The slope of the linear part of the plot corresponds to the motility coefficient, and was determined by linear regression analysis using GraphPad Prism data analysis software. The confinement distance was determined by visually identifying the plateau value. The first order rate constant for cells leaving confinement zones ( $k=0.0069$ , corresponding to a half-life of 100 minutes or 1.7 hours) was estimated based on a first-order rate equation  $-d[\text{cells}]/dt = k [\text{cells}]$ , where  $-d[\text{cells}] = 6$  (cells that left zones),  $dt = 13$  minutes (average track duration) and  $[\text{cells}] = 67$  (number of tracked cells in zones). For manual scoring of thymocyte-DC interactions, individual thymocytes tracks were inspected in 3D space at each time point by an unbiased observer and scored for time points in which visible contacts with DCs occurred<sup>19</sup>.

### Statistical Analysis

GraphPad Prism was used for graphing and statistical analysis. Unpaired t-tests were performed to compare the means of different data sets, except for paired data sets (e.g. samples from the same imaging volume), for which a pairwise t-test was used

### Antibodies and flow cytometry

OT1<sup>+</sup> *Rag2*<sup>-/-</sup> and OT1<sup>+</sup> *Rag2*<sup>-/-</sup> RIPmOVA<sup>+</sup> littermates were sacrificed at 4 week old. Thymocytes were stained with different combinations of the following antibodies (Abs): anti-CD8-FITC, -PECy5 or -PECy7 (clone 53–6.7); anti-V $\alpha$ 2 TCR-PE or – APC (clone b20.1); anti-CD4-PE-TxRed (clone RM4–5); anti-CD24-PE (clone M1/69) Abs (BD Biosciences and eBioscience). In some cases, cells were then fixed, permeabilized, and stained for active-caspase 3 as previously described<sup>28</sup>. Cell events were collected with a Beckman-Coulter FC-500 flow cytometer and analyzed with FlowJo software (Tree Star Inc.).

### Supplementary Material

Refer to Web version on PubMed Central for supplementary material.

### Acknowledgments

We thank H. Nolla (University of California Berkeley, Cancer Research Labs) for assistance with flow cytometry, the University of California Berkeley Molecular Imaging Center for microscopy, M. Anderson (University of California San Francisco) for providing RIPmOVA mice, L. Ehrlich and R. Lewis (Stanford University) for communication of unpublished data, and P. Bousso (Pasteur Institute, Paris, France), B.J. Fowlkes (National Institute of Health, Bethesda, MD), and members of the Robey Laboratory for comments on this manuscript.

### References

1. Kyewski B, Klein L. A central role for central tolerance. *Annu Rev Immunol.* 2006; 24:571–606. [PubMed: 16551260]
2. Anderson MS, et al. Projection of an immunological self shadow within the thymus by the aire protein. *Science.* 2002; 298:1395–1401. [PubMed: 12376594]
3. Mathis D, Benoist C. Aire. *Annu Rev Immunol.* 2009; 27:287–312. [PubMed: 19302042]
4. Derbinski J, Schulte A, Kyewski B, Klein L. Promiscuous gene expression in medullary thymic epithelial cells mirrors the peripheral self. *Nat Immunol.* 2001; 2:1032–1039. [PubMed: 11600886]
5. Anderson MS, et al. The cellular mechanism of Aire control of T cell tolerance. *Immunity.* 2005; 23:227–239. [PubMed: 16111640]
6. Liston A, Lesage S, Wilson J, Peltonen L, Goodnow CC. Aire regulates negative selection of organ-specific T cells. *Nat Immunol.* 2003; 4:350–354. [PubMed: 12612579]

7. Gallegos AM, Bevan MJ. Central tolerance to tissue-specific antigens mediated by direct and indirect antigen presentation. *J Exp Med*. 2004; 200:1039–1049. [PubMed: 15492126]
8. Bonasio R, et al. Clonal deletion of thymocytes by circulating dendritic cells homing to the thymus. *Nat Immunol*. 2006; 7:1092–1100. [PubMed: 16951687]
9. Donskoy E, Goldschneider I. Two developmentally distinct populations of dendritic cells inhabit the adult mouse thymus: demonstration by differential importation of hematogenous precursors under steady state conditions. *J Immunol*. 2003; 170:3514–3521. [PubMed: 12646612]
10. Gray D, Abramson J, Benoist C, Mathis D. Proliferative arrest and rapid turnover of thymic epithelial cells expressing Aire. *J Exp Med*. 2007; 204:2521–2528. [PubMed: 17908938]
11. Ohnmacht C, et al. Constitutive ablation of dendritic cells breaks self-tolerance of CD4 T cells and results in spontaneous fatal autoimmunity. *J Exp Med*. 2009; 206:549–559. [PubMed: 19237601]
12. McCaughy TM, Wilken MS, Hogquist KA. Thymic emigration revisited. *J Exp Med*. 2007; 204:2513–2520. [PubMed: 17908937]
13. Mempel TR, Henrickson SE, Von Andrian UH. T-cell priming by dendritic cells in lymph nodes occurs in three distinct phases. *Nature*. 2004; 427:154–159. [PubMed: 14712275]
14. Cahalan MD, Parker I. Choreography of cell motility and interaction dynamics imaged by two-photon microscopy in lymphoid organs. *Annu Rev Immunol*. 2008; 26:585–626. [PubMed: 18173372]
15. Bouso P, Robey E. Dynamic behavior of T cells and thymocytes in lymphoid organs as revealed by 2-photon microscopy. *Immunity*. 2004; 21:349–355. [PubMed: 15357946]
16. Bouso P, Bhakta NR, Lewis RS, Robey E. Dynamics of thymocyte-stromal cell interactions visualized by two-photon microscopy. *Science*. 2002; 296:1876–1880. [PubMed: 12052962]
17. Bhakta NR, Oh DY, Lewis RS. Calcium oscillations regulate thymocyte motility during positive selection in the three-dimensional thymic environment. *Nat Immunol*. 2005; 6:143–151. [PubMed: 15654342]
18. Witt CM, Raychaudhuri S, Schaefer B, Chakraborty AK, Robey EA. Directed Migration of Positively Selected Thymocytes Visualized in Real Time. *PLoS Biol*. 2005; 3:e160. [PubMed: 15869324]
19. Ladi E, et al. Thymocyte-dendritic cell interactions near sources of CCR7 ligands in the thymic cortex. *J Immunol*. 2008; 181:7014–7023. [PubMed: 18981121]
20. Lindquist RL, et al. Visualizing dendritic cell networks in vivo. *Nat Immunol*. 2004; 5:1243–1250. [PubMed: 15543150]
21. Schaefer BC, Schaefer ML, Kappler JW, Marrack P, Kiedl RM. Observation of antigen-dependent CD8+ T-cell/dendritic cell interactions in vivo. *Cell Immunol*. 2001; 214:110–122. [PubMed: 12088410]
22. Hadjantonakis AK, Macmaster S, Nagy A. Embryonic stem cells and mice expressing different GFP variants for multiple non-invasive reporter usage within a single animal. *BMC Biotechnol*. 2002; 2:11. [PubMed: 12079497]
23. Ladi E, Herzmark P, Robey E. In situ imaging of the mouse thymus using 2-photon microscopy. *J Vis Exp*. 2008
24. Miller MJ, Wei SH, Parker I, Cahalan MD. Two-photon imaging of lymphocyte motility and antigen response in intact lymph node. *Science*. 2002; 296:1869–1873. [PubMed: 12016203]
25. Kurts C, et al. Constitutive class I-restricted exogenous presentation of self antigens in vivo. *J Exp Med*. 1996; 184:923–930. [PubMed: 9064352]
26. Lucas B, Germain RN. Unexpectedly complex regulation of CD4/CD8 coreceptor expression supports a revised model for CD4+CD8+ thymocyte differentiation. *Immunity*. 1996; 5:461–477. [PubMed: 8934573]
27. Lundberg K, Heath W, Kontgen F, Carbone FR, Shortman K. Intermediate steps in positive selection: differentiation of CD4+8int TCRint thymocytes into CD4+8+TCRhi thymocytes. *J Exp Med*. 1995; 181:1643–1651. [PubMed: 7722444]
28. McCaughy TM, Baldwin TA, Wilken MS, Hogquist KA. Clonal deletion of thymocytes can occur in the cortex with no involvement of the medulla. *J Exp Med*. 2008; 205:2575–2584. [PubMed: 18936237]

29. Jung S, et al. In vivo depletion of CD11c(+) dendritic cells abrogates priming of CD8(+) T cells by exogenous cell-associated antigens. *Immunity*. 2002; 17:211–220. [PubMed: 12196292]
30. Apostolou I, Sarukhan A, Klein L, von Boehmer H. Origin of regulatory T cells with known specificity for antigen. *Nat Immunol*. 2002; 3:756–763. [PubMed: 12089509]
31. Haribhai D, et al. Regulatory T cells dynamically control the primary immune response to foreign antigen. *J Immunol*. 2007; 178:2961–2972. [PubMed: 17312141]
32. Bousso P. T-cell activation by dendritic cells in the lymph node: lessons from the movies. *Nat Rev Immunol*. 2008; 8:675–684. [PubMed: 19172690]
33. Surh CD, Sprent J. T-cell apoptosis detected in situ during positive and negative selection in the thymus. *Nature*. 1994; 372:100–103. [PubMed: 7969401]
34. Kappler JW, Roehm N, Marrack P. T cell tolerance by clonal elimination in the thymus. *Cell*. 1987; 49:273–280. [PubMed: 3494522]
35. Derbinski J, Pinto S, Rosch S, Hexel K, Kyewski B. Promiscuous gene expression patterns in single medullary thymic epithelial cells argue for a stochastic mechanism. *Proc Natl Acad Sci U S A*. 2008; 105:657–662. [PubMed: 18180458]
36. Baldwin TA, Sandau MM, Jameson SC, Hogquist KA. The timing of TCR alpha expression critically influences T cell development and selection. *J Exp Med*. 2005; 202:111–121. [PubMed: 15998791]
37. Akiyama T, et al. The tumor necrosis factor family receptors RANK and CD40 cooperatively establish the thymic medullary microenvironment and self-tolerance. *Immunity*. 2008; 29:423–437. [PubMed: 18799149]
38. Hikosaka Y, et al. The cytokine RANKL produced by positively selected thymocytes fosters medullary thymic epithelial cells that express autoimmune regulator. *Immunity*. 2008; 29:438–450. [PubMed: 18799150]
39. Irla M, et al. Autoantigen-specific interactions with CD4+ thymocytes control mature medullary thymic epithelial cell cellularity. *Immunity*. 2008; 29:451–463. [PubMed: 18799151]
40. Schaefer BC, Schaefer ML, Kappler JW, Marrack P, Kiedl RM. Observation of antigen-dependent CD8+ T-cell/dendritic cell interactions in vivo. *Cell Immunol*. 2001; 214:110–122. [PubMed: 12088410]

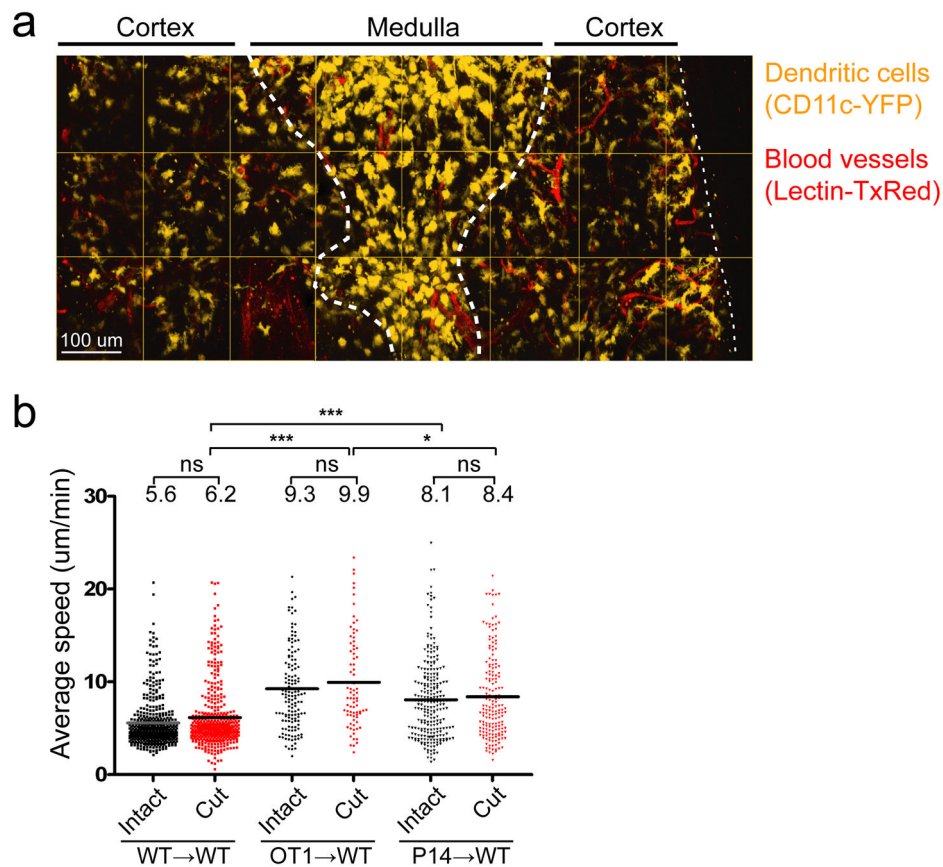


**Figure 1. Sectioning the thymus facilitates imaging of the medulla**

**a.** The thymus of a CD11c-YFP<sup>+</sup> mouse, injected with lectin-Texas Red before sacrifice to label blood vessels, was cut and imaged by two-photon microscopy. Image shows a montage of maximal projections of adjacent 3D data sets spanning the cut thymus from the dorsal to the ventral side. Scale bar indicates 100  $\mu$ m. Image is representative of more than 20 cut thymuses. **b.** Plot shows the average speed of individual thymocyte tracks in the cortex of an intact or a cut thymic lobe. Each dot represents the average speed of an individual track. For each population, the mean average speed is listed at the top of each column. This analysis was based on data for at least 3 individual chimeras with 449 WT  $\rightarrow$  WT tracks from intact thymic lobes and 443 from cut thymic lobes, 142 OT1  $\rightarrow$  WT tracks from intact thymic lobes and 88 tracks from cut thymic lobes, and 244 P14  $\rightarrow$  WT tracks from intact thymic lobes and 174 tracks from cut thymic lobes. *ns* (not significant),  $P > 0.05$ ; \*,  $0.01 < P < 0.05$ ; \*\*\*,  $P < 0.001$ .



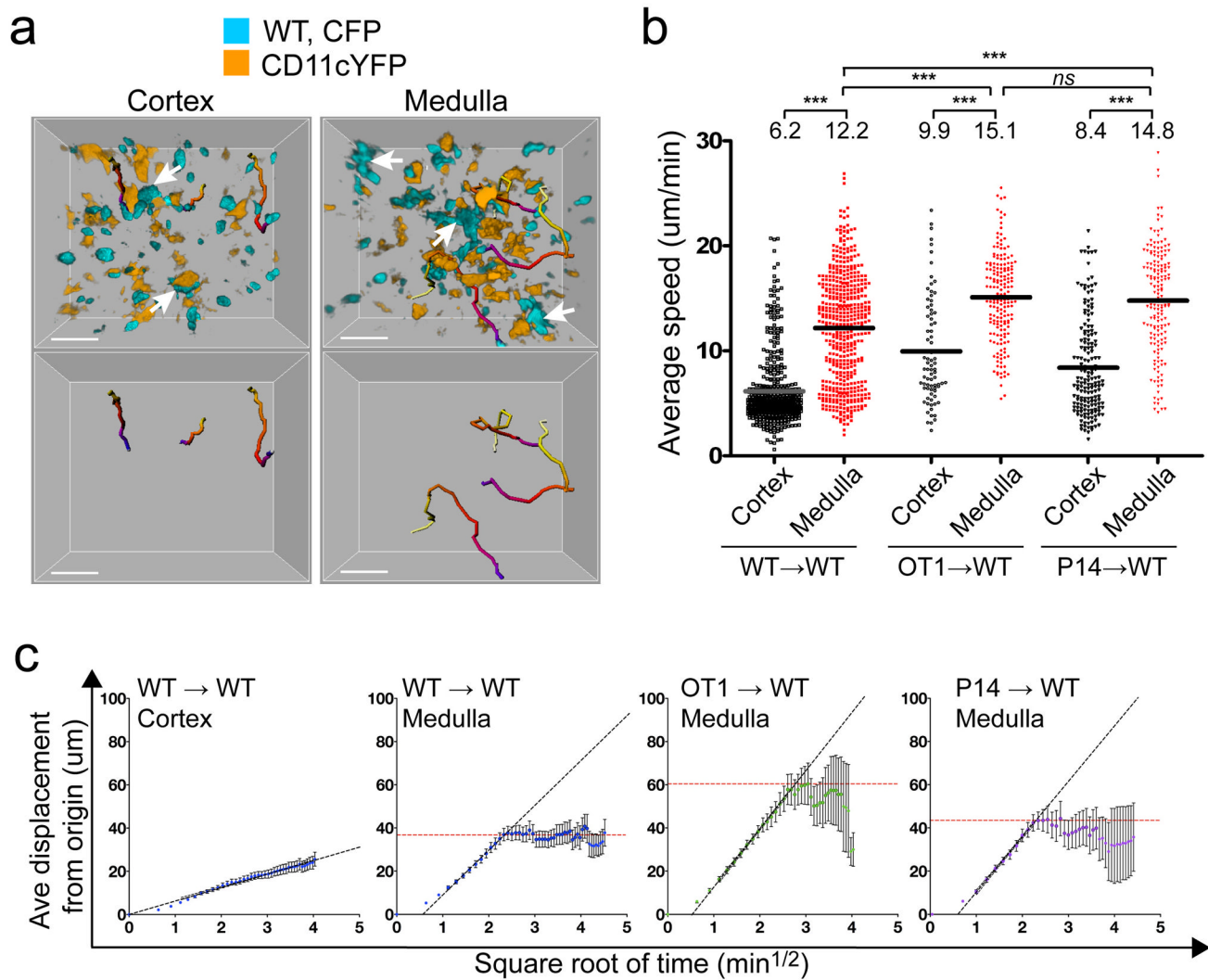


**Figure 2. Thymocyte migration in the medulla is rapid and confined**

**a.** Representative stills of two-photon imaging volumes in the cortex or the medulla of a cut thymic lobe with WT CFP-labeled thymocytes and CD11c-YFP<sup>+</sup> DCs. Three representative tracks with the duration of 10.4 min are color-coded for time (blue > red > yellow). White arrows indicate donor-derived, CFP<sup>+</sup> DCs. Scale bar indicates 30  $\mu$ m. **b.** Each dot represents the average speed of an individual tracked thymocyte, in the cortex or the medulla of WT  $\rightarrow$  WT, OT1  $\rightarrow$  WT or P14  $\rightarrow$  WT chimeras. At the top of each column, the mean average\_speed is listed for each population. This analysis was based on data for 443 WT  $\rightarrow$  WT cortical tracks from 6 chimeras, 505 WT  $\rightarrow$  WT medullary tracks from 6 chimeras, 80 OT1  $\rightarrow$  WT cortical tracks from 3 chimeras, 183 OT1  $\rightarrow$  WT medullary tracks from 3 chimeras, 174 P14  $\rightarrow$  WT cortical tracks from 3 chimeras, and 171 P14  $\rightarrow$  WT medullary tracks from 3 chimeras. *ns*,  $P > 0.05$ ; \*\*\*,  $P < 0.001$ . **c.** The average displacement from origin is plotted as a function of the square root of time for representative runs from indicated chimeras. Graphical view of linear regression analysis for the sloped regions of each plot (black dotted line) and the estimated plateaus (red dotted line) are shown. Error bars indicate s.e.m.

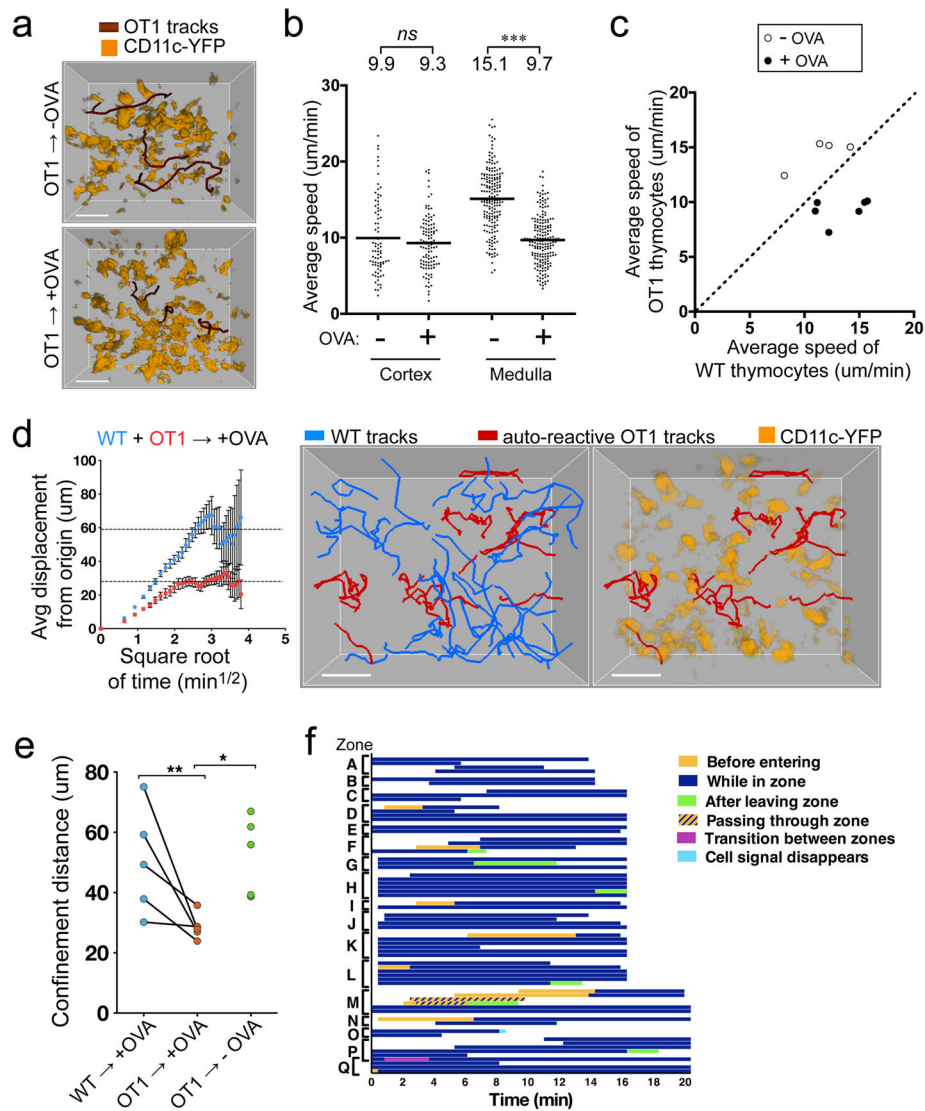


**Figure 3. The impact of negative selection on thymocyte migration**

**a.** Two-photon imaging volumes in the medulla show CD11c-YFP<sup>+</sup> cells and 3 representative OT1 thymocyte tracks with durations of 12.5 min in hosts without or with OVA. Scale bar indicates 30 μm. **b.** Average speeds of OT1 thymocytes in the cortex and the medulla in hosts with or without OVA. For each population, mean average speeds is indicated at the top of each column. Runs from 3 OT1+WT → -OVA chimeras (80 cortical tracks and 183 medullary tracks) and 5 OT1+WT → +OVA chimeras (105 cortical tracks and 187 medullary tracks) were analyzed. *ns*,  $P > 0.05$ ; *\*\*\**,  $P < 0.001$ . **c.** Compiled data from the medulla showing the mean average speed for OT1 thymocytes versus WT thymocytes from the same run. Each dot represents an individual imaging volume from OT1+WT → -OVA chimeras and OT1+WT → +OVA chimeras. **d.** Left plot shows average displacement from origin against the square root of time for WT and OT1 thymocytes for a representative OT1+WT → +OVA chimera. Black dotted lines indicate plateau values and error bars indicate s.e.m. OT1 thymocyte tracks are shown with polyclonal thymocytes tracks (middle panel) or CD11c-YFP-labeled DCs (right panel). **e.** Graph shows confinement distances of WT and OT1 thymocytes from WT+OT1 → +OVA

chimeras (lines connect values from the same imaging volumes) and OT1  $\rightarrow$  -OVA chimeras. \*,  $0.01 < P < 0.05$ ; \*\*,  $0.001 < P < 0.01$ . **f.** Migration of auto-reactive thymocytes from OT1+WT  $\rightarrow$  +OVA chimeras into and out of confinement zones. Horizontal lines represent 67 OT1 thymocytes (5 runs) whose tracks defined 17 confinement zones (A–Q).

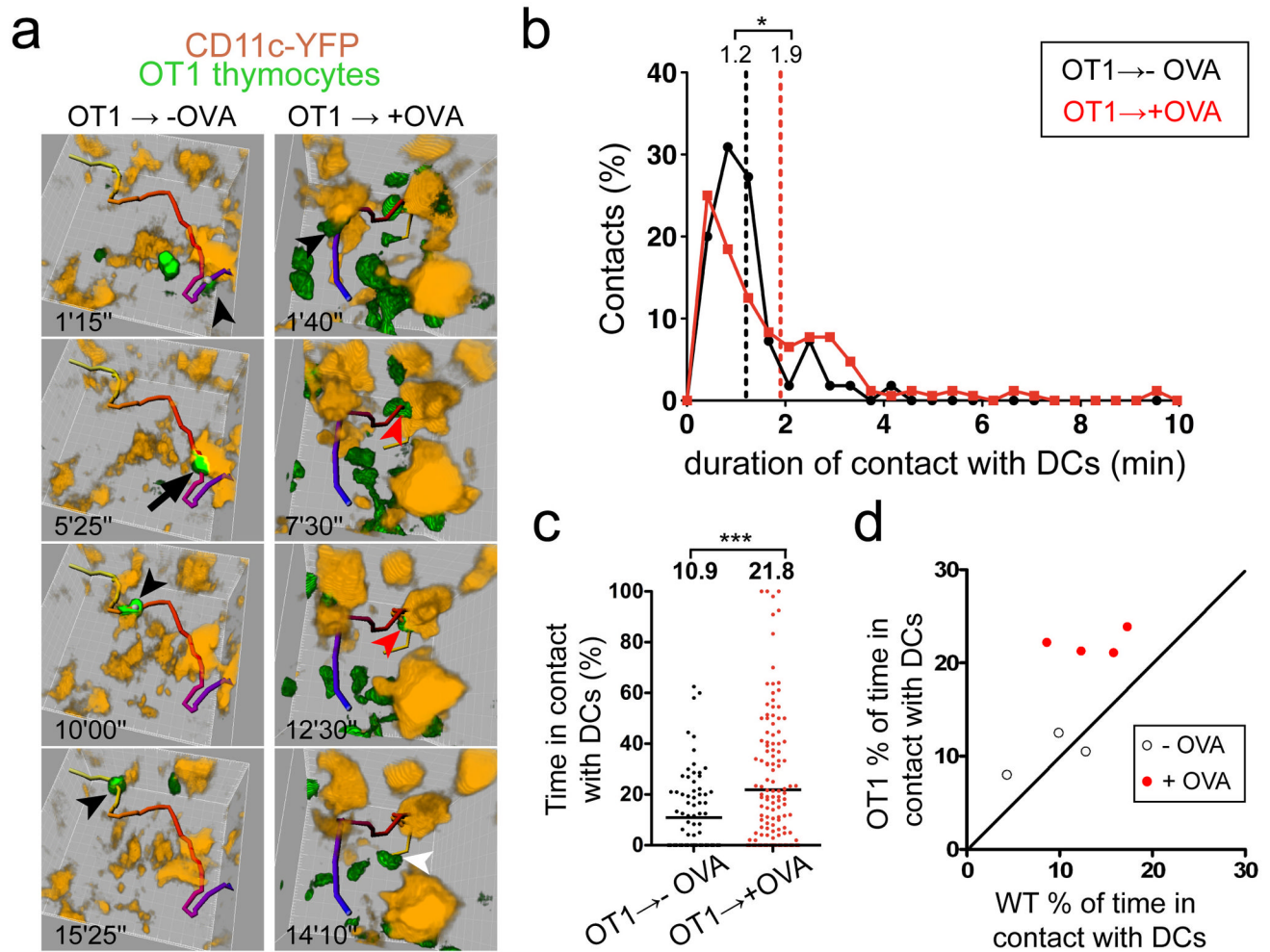


**Figure 4. Increased thymocyte-DC interactions during negative selection**

**a.** Examples of OT1 GFP thymocytes that make successive interactions with CD11c-YFP<sup>+</sup> DCs in hosts in the presence or absence of OVA. Thymocyte tracks are color-coded to indicate the passage of time (blue at the start of imaging to white at the end). Thymocyte-DC contacts are indicated with a black arrowhead while the absence of a contact is indicated with a white arrowhead. Close contacts in OT1 thymocyte from OT1 → -OVA chimeras are shown with a black arrow while red arrowheads in OT1 thymocyte from OT1 → +OVA chimeras indicate long lasting contact with a DC. **b-c.** Interactions between DCs and OT1 thymocytes in the medulla in the presence or absence of OVA. Tracks for individual thymocytes were monitored in intervals of 25 seconds, and the number of time points during which each thymocyte contacted a DC was recorded. The graphs show **(b)** the relative frequency of contacts of indicated duration, and **(c)** the percent of time each thymocyte spent in contact with DCs. Mean values listed at top of graph.  $P > 0.05$ ; \*,  $0.01 < P < 0.05$ ; \*\*\*,  $P < 0.001$ . **d.** Compiled data showing the mean % of time that wild-type thymocytes spent in contact with DCs versus the mean % of time that OT1 thymocytes spent in contact with DCs in the same imaging volume. Each dot represents an individual TPSLM run. Imaging volumes from 3 OT1+WT → -OVA chimeras and 5 OT1+WT → +OVA chimeras were analyzed.

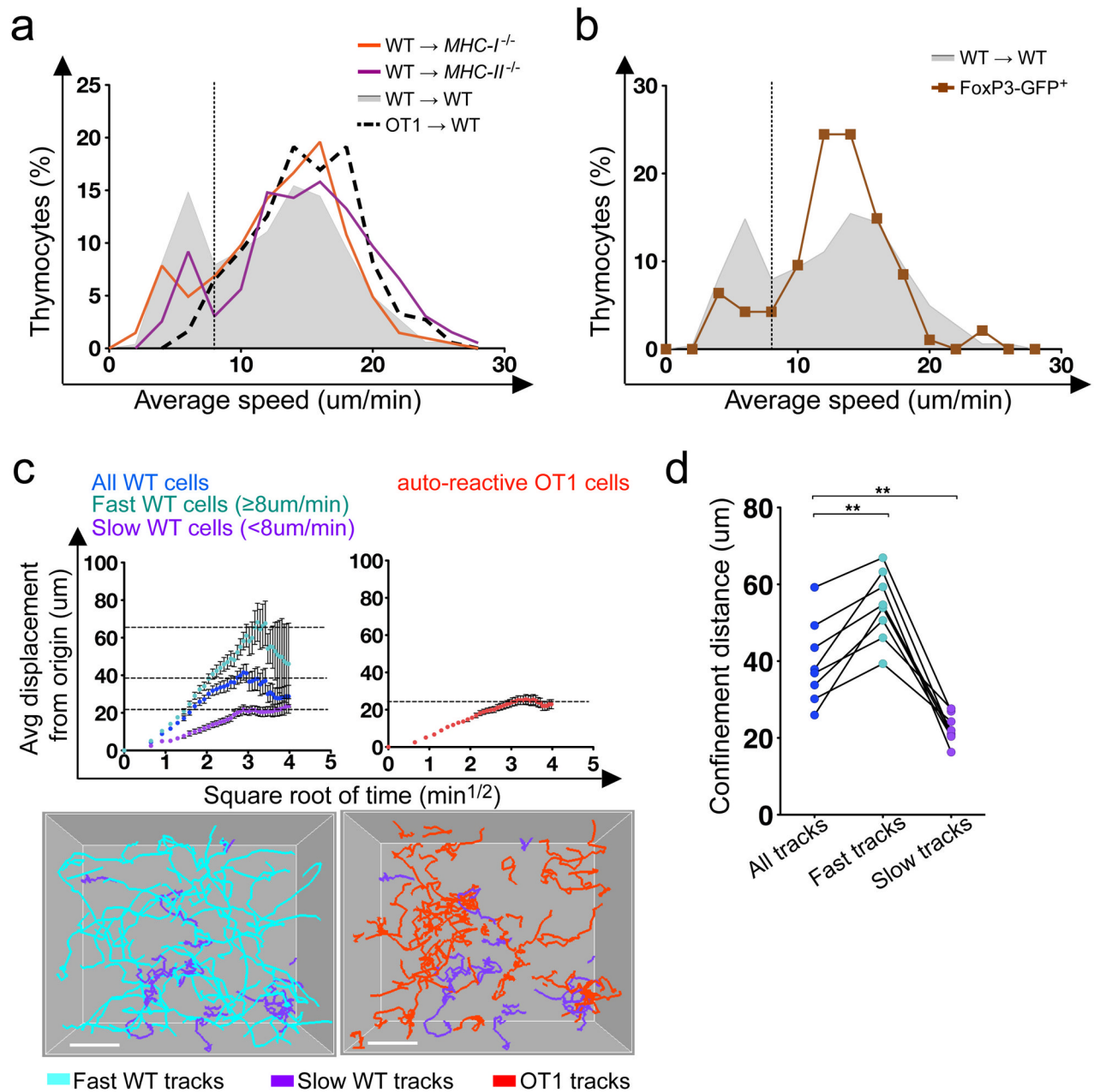


**Figure 5. A subset of polyclonal medullary thymocytes exhibits slower, more confined migration**  
**a–b.** Relative frequency distribution of average speeds of medullary thymocytes from indicated chimeras (**a**,**b**) or of GFP<sup>+</sup> thymocytes in Foxp3-GFP reporter mice (**b**). The differences between the mean average speed of WT → WT and WT → *MHC-I*<sup>-/-</sup> thymocytes or Foxp3-GFP<sup>+</sup> thymocytes were not significant ( $P > 0.05$ ) whereas the difference between WT → WT and WT → *MHC-II*<sup>-/-</sup> thymocytes was significant ( $P < 0.001$ ). Vertical dotted line indicates the cut-off used to define slow versus fast medullary thymocytes (8  $\mu\text{m}/\text{min}$ ). Imaging volumes from 3 WT → *MHC-I*<sup>-/-</sup> chimeras (204 tracks), 2 WT → *MHC-II*<sup>-/-</sup> (196 tracks), 6 WT → WT (183 tracks), and 3 Foxp3-GFP reporter mice (94 tracks) were analyzed. **c.** Graphs show average displacement against the square root of time of thymocytes in WT + OT1 → +OVA chimeras. Left, wild-type thymocytes



with average speeds of  $\geq 8 \mu\text{m}/\text{min}$ ,  $<8 \mu\text{m}/\text{min}$ , or all cells. Right, OT1 thymocytes from the same imaging volumes. Dashed lines indicate estimated plateau of confined migration for each curve. Error bars indicate s.e.m. Plots show tracks of fast and slow WT thymocytes compared to OT1 thymocytes. Scale bar,  $30 \mu\text{m}$ . Imaging volumes from 5 OT1+WT  $\rightarrow$  +OVA chimeras were analyzed. **d.** Size of confinement distance for WT thymocytes for all tracks,  $\geq 8 \mu\text{m}/\text{min}$ , and  $<8 \mu\text{m}/\text{min}$ . Data are from 5 WT+OT1  $\rightarrow$  +OVA and one WT+OT1  $\rightarrow$  -OVA chimeras. Lines connect values from the same imaging volumes and significance was calculated using paired t-tests. \*\*,  $0.001 < P < 0.01$ .